Journal of Interfaces, Thin films, and Low dimensional systems 6 (1) Summer and Autumn (2022) 591-602

Correlation of heat treatment and structural, optical, and electrical properties of titanium nitride thin layers

Scientific research paper

Somayeh Asgary*, Zhaleh Ebrahiminejad, Amir Hoshang Ramezani

Department of Physics, West Tehran Branch, Islamic Azad University, Tehran, Iran

ARTICLE INFO

Article history:
Received 5 January 2023
Revised 12 April 2023
Accepted 27 April 2023
Available online 29 June 2023

Keywords
TiN films
DC magnetron sputtering
Preferred growth orientation

ABSTRACT

TiN thin films are prepared by the DC magnetron sputtering method, and the effect of post annealing treatment on the physical, structural, morphological, and optical properties of TiN layers are investigated by X-ray diffraction (XRD), scanning electron microscopy (SEM), atomic force microscopy (AFM), and UV-VIS spectrophotometer. Variation of electrical resistivity and film's hardness are also investigated. Based on the XRD results, increasing annealing temperature would not change film's stoichiometry, but deteriorates improvement of the films crystalline quality. The as-deposited film with amorphous structure changes to a single-phase crystalline structure that has a preferred orientation along (111) and the polycrystalline structure at higher annealing temperatures. According to SEM images, a dense structure transforms to a denuded zone structure during annealing temperature. The reflectance of TiN films shows a minimum in the visible region indicating a significant increase in the infrared region. The optical band gap energy value increases by increasing the annealing temperature while, the electrical resistivity and hardness values decrease.

1 Introduction

Transition-metal nitride coatings are currently used in an extensive variety of applications because of their unique physical, chemical, mechanical, electrical, and optical properties such as excellent bond strength to the substrate [1-2], high scratch and abrasion resistance [3], low friction coefficient [4], good chemical inertness, high-temperature oxidation resistance [5], high thermal stability, high melting point [6], electrical conductivity alternating from metallic to semiconducting, [7], high optical transmittance in the visible spectrum (with thickness of less than 30 nm) [6], high optical reflectance in the infrared (IR) spectrum, superconductivity [8], superior irradiation resistance and high hardness [9].

Transition-metal can bond with nitrogen and form binary nitride compounds. Among them, TiN films have great interest in engineering and are beneficial for various applications in hard coatings as protective material for cutting tools and machine parts [10], diffusion barriers in microelectronic devices [11], gate electrodes in field-effect transistors and flat panel displays [12], photo-thermal solar energy conversion coating [13], semi-transparent contacts in solar cells [14] , ohmic contacts on III-nitride semiconductors [15], Schottky contacts on Si [16], rectifying contact for p- GaN [17], high temperature heterogeneous catalysis [18], anti-corrosion coatings [19], thin film resistors, optical filters [17], and decorative coatings in architecture due to its bright golden color [20]. Also, TiN is used in medical applications as medical implants (orthopedic and dental prosthesis) [21] because of its

*Corresponding author.
Email address: Sima198124@Yahoo.com
DOI: 10.22051/jitl.2023.42338.1078

biocompatible properties [22], high hardness and high ductility.

Ti-N is a chemically inert refractory compound. It characterizes in different phases such as TiN, Ti_2N, and Ti_3N_4 [23] but, the cubic rock salt B_1-TiN structure is the most stable phase among them that is also called δ-TiN [24]. TiN is a solid solution with nitrogen (the nitrogen concentration is about 37.5%-50%) [25].

Several researchers have studied the properties of TiN thin layers [26-27]. These layers have been fabricated by many different methods such as chemical vapor deposition (CVD) [28], metal-organic chemical vapor deposition (MOCVD) [6], plasma enhanced chemical vapor deposition (PECVD), low temperature plasma treatment with N_2 plasma [29], ion beam assisted deposition [30], electron beam, cathodic vacuum arc [31], sol-gel, pulsed laser deposition [32], high power impulse magnetron sputtering [33], electron cyclotron resonance plasma chemical vapor deposition [6], dip-coating, atomic layer deposition [34], thermal oxidation and magnetron sputtering [35] to study the growth of TiN layers in order to understand and control their microstructural features like type of growth (columnar or globular), orientation, grain size, etc. [36].

Thin films with different crystallographic structure and morphology with different physical properties can be produced by sputtering technique. This method has advantages such as low levels of impurities in the deposited thin films and easy control of deposition rate [37].

Hofmann reported the deposition of TiN by sputtering titanium targets in Ar/N_2 plasma mixtures [38]. Mientus and Ellmer studied the fabrication of nitrides at different nitrogen partial pressures [39]. Investigation of deposited TiN films by using DC magnetron sputtering method at 300-400°C is reported by [40-41]. Vasua et al. studied the deposition of TiN thin films by RF reactive magnetron sputtering method in 100% nitrogen atmosphere [42]. Also, a good stoichiometry TiN thin layer is deposited by heating up to 600°C [17].

In this work, we employed DC reactive magnetron sputtering for deposition of TiN thin films. Then, deposited thin films were post annealed in the air condition at different annealing temperatures. The influences of annealing treatment on the structural, morphological, optical, electrical, and mechanical properties and of TiN thin films were investigated.

Thermal annealing after deposition can improve the film's microstructure and optimize their physical properties by reducing defects and residual stresses [43]. The changes in TiN coatings microstructure after heat treatment annealing process are reported in other literatures. Mayrhofer et al. [44] showed the influence of annealing treatment on crystallographic orientation and the grain size of nanocrystalline TiN thin films deposited by the unbalanced magnetron sputtered technique. Similar study relating to the effect of annealing process on the crystallinity, texture, and grain size was investigated by Huang et al. [13].

2 Experimental details

A DC reactive cylindrical magnetron sputter deposition unit was used as the sputtering system in this work. The system consists of a cylindrical Ti metal (99.99 % pure) as a target (cathode) 2 cm radius and a cylindrical aluminum metal as a sample sustainer (anode) with 5 cm radius. The height of the anode and cathode was 20 cm. The n-type silicon wafers and quartz substrates were cleaned ultrasonically by using acetone, alcohol, and deionized water about 10 min for each step. The Ti target was placed in the center of the growth setup. The growth chamber was evacuated by using a diffusion pump backed with a rotary pump (ALCATEL) to produce a vacuum of 2×10^{-5} Torr. The working pressure for sputtering was 2×10^{-2} Torr. For better adhesion, we injected the pure argon gas into the chamber to deposit a thin Ti layer (with about 10 nm thick) on the cleaned substrates. Then without breaking the vacuum, we used a mixed gas of 95% argon+ 5% nitrogen for TiN deposition on the Ti films.

The magnetron was created by a ring shape of permanent magnet placed in the gun behind the target attachment surface. The constant magnetron current for deposition was 0.28 A, with a discharge voltage of 600 V. The deposition conditions were listed in Table 1. The schematic of a DC magnetron sputtering system is given in Fig. 1.

The chemical composition of the TiN thin film is influenced by deposition conditions and amount of reagents in the substrate plane, with the following formulas:

$Ti + N_2 = TiN + 0.5N_2$, (1)

$2Ti + N_2 = 2TiN$, (2)

$3Ti + N_2 = Ti_2N + TiN$, (3)

$4Ti + N_2 = Ti_2N + TiN + Ti$. (4)

Based on the Ti-N phase diagram [45], in addition to TiN phase, Ti_2N can be formed as second phase. The composition of deposited coating is determined by the rate of titanium condensation on the substrate, N_2 partial pressure and the degree of ionization (generally the degree of condensation in the working chamber) is not uniform in all regions [46].

The deposited coatings were post annealed in the air condition for 60 min at different temperatures of 400, 500, 600, and 700°C.

The crystalline structures of deposited thin films are studied by using STOE SIADI MP X-ray diffractometer for 2θ values up to 80° with Cu K_α radiation (1.5405 Å) as the source of X-ray radiation.

Table 1. Deposition parameters

Substrate-to-target distance (mm)	35
Substrates	Si, Quartz
Base pressure (Torr)	2×10^{-5}
Work pressure (Torr)	2×10^{-2}
Voltage (Volt)	600
Current (mA)	3.5
Deposition time for Ti (min)	10
Deposition time for TiN (min)	40

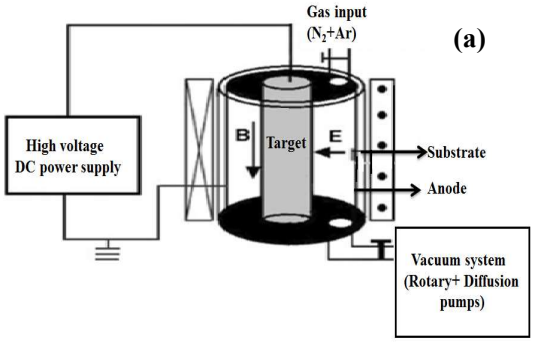

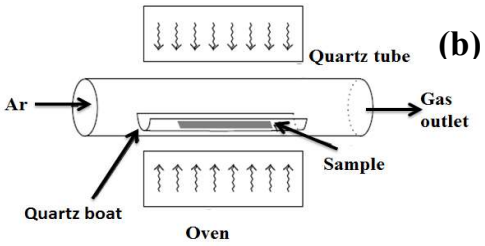

Figure 1. Schematic diagram of (a) DC cylindrical magnetron sputtering and (b) Oven.

The surface roughness of the films is measured by an atomic force microscope (AFM) and the surface micrographs were performed by using the Park scientific scanning electron microscopy (SEM) system and optical properties were studied by using Perkin–Elmer Lambda 950 spectrophotometer in the wavelength range UV-VIS (10–2500 nm) at room temperature. Electrical resistivity of deposited thin films is investigated by the four-point probe technique at room temperature. Hardness is determined using the ASTM E92-IS0 6507 tester.

3-Results and discussion

3.1 X ray diffraction results

The crystal structures of annealed TiN thin films are studied by X-ray diffraction (XRD) operating in Bragg-Brentano θ/2θ configuration using a Cu K_α wavelength (1.5418 Å) working at 30 kV and 20 mA.

The as-deposited films show amorphous phase (Fig. 2) but after annealing for 1 hour the films transformed into the crystalline. Figure 3 shows the XRD pattern of thin films after annealing at different temperatures for 1 hour. The XRD pattern shows variation of annealing temperature effects on intensity and preferred orientation of peaks. The crystallographic structure depends on the annealed temperature. The peak intensity varies with the scattering intensity of the crystalline structure components, the atoms, molecules, and their arrangement in the lattice [47]. High intensity indicates the more orders of the crystallization and arrangement.

The sharp peak at 2θ = 36.87° for annealed films (400 and 500°C), is correlated to the (111) crystallographic orientations of TiN with a face-centered cubic (FCC) structure (JCPDS: 38-1420). The FCC structure of TiN

can be arranged when nitrogen atoms occupy all the octahedral sites of titanium with hexagonal close-packed (HCP) or body centered cubic (BCC) structures [6]. The diagram phase of titanium–nitrogen is complex; because nitrogen atoms with smaller size can accommodate in the interstitial sites of titanium structure with larger size [48].

With increasing the annealing temperature to 600°C, several new reflection peaks appear at 2θ = 42.54°, 61.88°, and 78.41° corresponding to (200), (220), and (222) planes, respectively, confirming of the construction of polycrystalline films. The half-width of the (111) x-ray diffraction peak is decreased. The sharp diffraction peaks indicate the large size of grains. The absence of the peaks related to the titanium crystalline structure in the XRD pattern shows that the nitride formation process has been completed.

When annealing temperature reached 700°C, the (220) peak intensity became stronger while the (111) peak intensity strongly reduced.

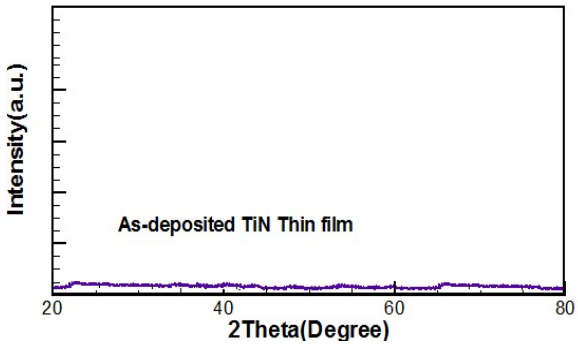

Figure 2. As-deposited thin film.

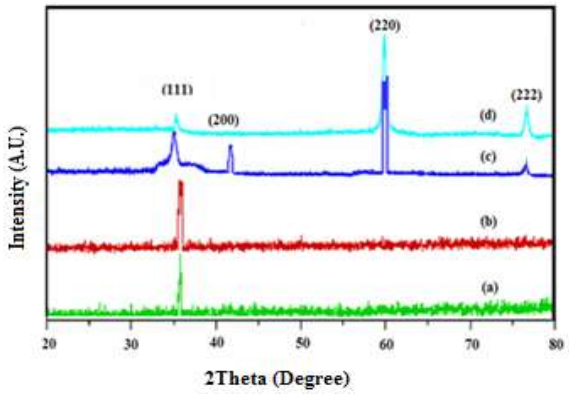

Figure 3. X-ray diffraction patterns of samples at different temperatures, (a) 400, (b) 500, (c) 600, and (d) 700°C.

At lower annealing temperatures, the relative intensity of the (111) diffraction peak is much higher in contrast to others, suggesting that (111) diffraction line is the preferred orientation with lowest energy. Competition between different parameters like, the surface energy, the strain energy, and the stopping energy of different lattice planes influences the preferred growth orientation and lowest total energy of the film [49].

In the annealing treatment from 400 to 500°C, the (111) preferred orientation did not change but the peak intensity is relatively increased. In fact, thermal energy created by post annealing treatment leads to improvement of mobility of active sites. Increasing the mobility may be due to grain growth and defects reduction through the annealing treatment [50].

We can note the existence of an additional TiN (200) phase in films annealed at 600°C that is not observed in other samples. The crystalline orientation of the deposited films depends on the film's growth process and a generalization of the behavior cannot be made very easily. The crystal orientation is also reliant on the surface free energy [51].

It is noted that at higher annealing temperatures, the preferred growth orientation changed from (111) to (220). With rising annealing temperature, the (220) plane is the primary orientation.

It is evident that a slight shift towards lower diffraction angles in the (111) diffraction peak position with increasing annealing temperature, corresponds to an expansion in the lattice constant that causes a compressive stress in the thin films.

3.2 SEM

The morphological and microstructure of the annealed TiN thin films have also been studied using the SEM analysis. Figs. 4a-4d shows the plane view of SEM images of deposited TiN thin films on Si substrate and annealed at different temperatures.

The SEM images showed homogenous coverage of the substrates by the TiN thin film. Significant differences in film's morphology were detected in the SEM images of annealed films at different temperatures.

The annealed films at 400°C and 500°C have particularly dense and very compact structure with non-

uniform surface. However, this feature is turned to discontinuous form with increasing annealing temperature to 600°C and 700°C with rough surface and some deep pores. It seems that with increasing the annealing temperature, the continuous feature is damaged and the TiN-denuded zone is observed that may be due to depleting TiN atoms from the surface (Fig. 3d).

It is evident that the microstructure evolution of TiN thin films is dependent on the annealing temperature. When the annealing temperature increases to higher values, the very compact and dense structure transformed to a denuded zone structure. It is apparent that the microstructure evolution of TiN thin films is dependent on the annealing temperature.

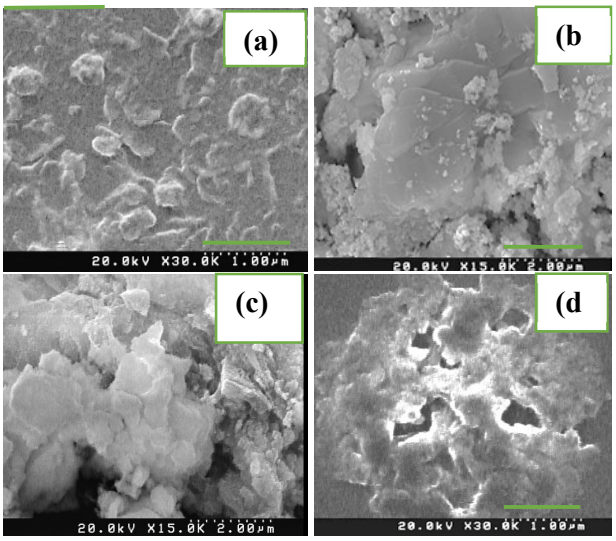

Figure 4. FE-SEM images of annealed thin films at different temperatures; (a) 400°C, (b) 500°C, (c) 600°C, and (d) 700°C.

3.3 AFM results

By using an atomic force microscope (AFM) analyzes, we have studied the film's surface morphology at different temperatures. Figure 5 shows 2D and 3D topography of the surface of the annealed films. All images are found in a scanning area of 1μm×1μm.

The annealed film at 400°C shows a continuous and dense morphology with the lowest RMS roughness. This film has a granular texture. Surface topography for the annealed film at 400°C shows a lower distribution of sparse clusters.

The topography of the annealed film at 500°C shows a relatively non-uniform surface distributed with heterogeneously spherical shape grains.

When the annealing temperature increases, the surface of the thin films become more non-uniform. Also, large sparse clusters appear on the film's surface. So, a rougher and coarser surface is observed at higher annealing temperature in our work.

The most usually reported measurement of film's surface roughness is the root mean square (RMS) roughness that is the standard deviation of the surface height profile from the average surface height. RMS roughness for annealed samples at 400-700°C is 1.88, 2.87, 2.98, and 3.46 nm, respectively.

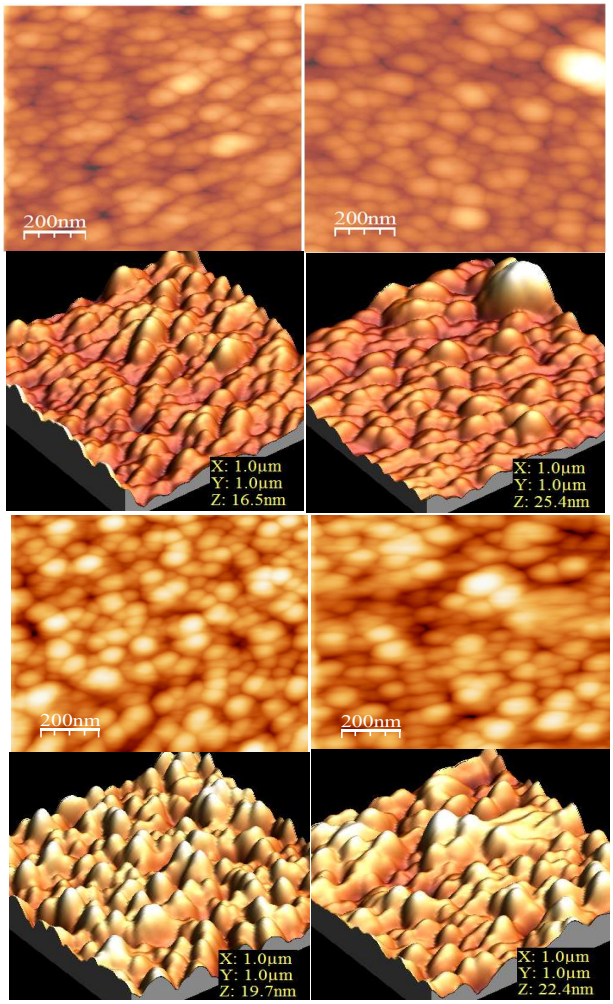

Figure 5. 2D and 3D AFM images of annealed films at different temperatures, (a) 400°C, (b) 500°C, (c) 600°C, and (d) 700°C.

The surface roughness of TiN thin films increased by increasing the post annealing temperature from 400°C to 700°C.

Figure. 6 shows the number of events diagrams as a function of surface topography variation. The topography curve of the annealed TiN thin films derived from AFM data indicates information about the distribution of particle size. The maximum of curve displays the nanoparticle average radius and width of the curve displays the change of particle radius size.

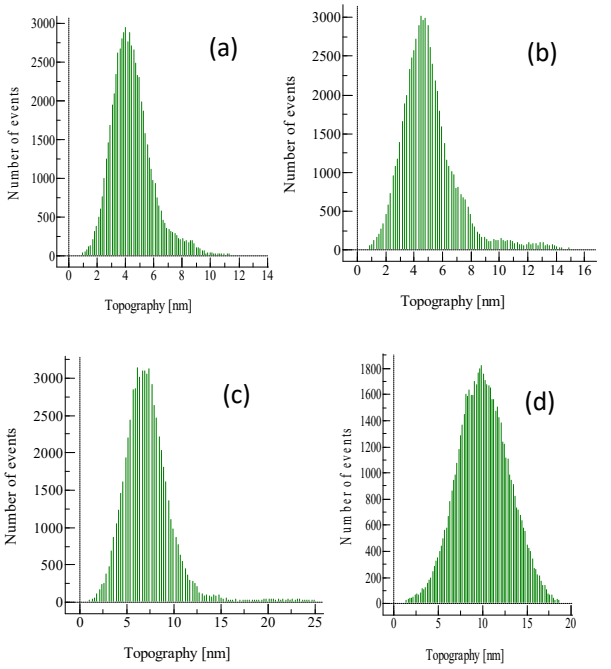

Figure 6. Number of events diagrams as a function of surface topography variations.

3.4 Optical properties

The reflectance spectra of annealed TiN thin films in the wavelength range 10-1200 nm is shown in Fig. 7. With increasing annealing temperature, the reflectance percentage increased in the visible region and saturated at about 85% in the near infrared region. In the ultraviolet region, the reflectance is less than 5% for all films. The TiN films reflectance spectra show a minimum in the visible region, while the reflectance increases in the infrared region. The reflectance minimum for stoichiometric TiN is detected centered around 2.33 eV, which corresponds to charge transfer between the Ti_{3p} and N_{2s} states [52]. The minimum reflectivity in the range of 450-460 nm is reported by Lousa et al. [53]. According to Guler et al. and Newport et al. [54-55] a low reflection peak in the range of 350–600 nm is observed for TiN films. However, in the entire wavelength region, the reflectance is higher for the annealed films at higher temperatures. Generally, increase in the reflectance can be recognized by structural transformation, film's surface roughness, and increasing grain size. Surface roughness strongly affects the thin film transparency. The main reason for increasing reflection at higher post annealing temperatures can be related to the scattering from rough surfaces. Light scattering from grains with irregular shapes or grain aggregates affect the films reflection.

These annealed thin films at different temperatures show a minimum in reflection spectra from blue region to ultraviolet and the high infrared reflection that displays the characteristics of a free electron metals as defined in the Drude model [56]. Because of the high reflectance at infrared region, TiN thin films have useful applications in solar absorbers at high temperatures, selectively transparent coatings, and energy-saving window films [57].

The optical absorption coefficient (α) of the films are calculated from the transmittance (T%) and reflectance (R%) spectra measurements using the following equation [58]:

$$\alpha = \frac{1}{d} \ln\left(\frac{(1-R)^2 + \sqrt{(1-R)^2 + (2RT)^2}}{2T}\right). \quad (5)$$

Here, d is the thickness of the films.

The optical band gap (E_g) can be calculated from the absorption coefficient by the following equation:

$$(\alpha h\upsilon)^n = A(h\upsilon - E_g), \quad (6)$$

where n = ½ for an indirect transmission [59]. The optical band gap energy of the deposited thin films can be calculated from the Tauc plot of $(\alpha h\upsilon)^{1/2}$ against the photon energy [60]. It can be considered from the best linear approximation of $(\alpha h\upsilon)^2$ against $(h\upsilon)$ plot, and its extrapolation to $(\alpha h\upsilon)^2 = 0$.

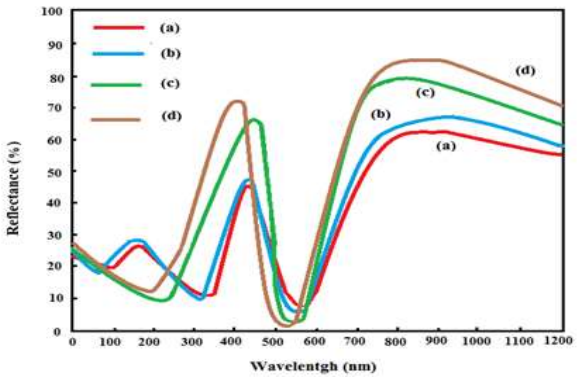

Figure 7. Reflectance spectrum for annealed TiN thin films at different temperatures. (a) 400°C, (b) 500°C, (c) 600°C, and (d) 700°C.

The reflectance spectra of TiN films show relatively similar features but an increase in reflection is observed with increasing the annealing temperature that can be attributed to different parameters such as structural transformation, increasing grain, size and surface roughness. The surface roughness strongly affects the film's transparency [61]. In our work, the major reason for the increase in reflection with higher annealing temperature may be due to the rough surface scattered and reflected light, as surface roughness increases upon annealing.

Figure 8 displays the optical band gap energy of the deposited TiN thin films as a function of the post annealing temperature. The optical band gap energy value of the annealed thin films can be different between 1.37 to 2.55 eV. The variance in the band gap energy values with post annealing temperatures is well correlated with the other studies [62].

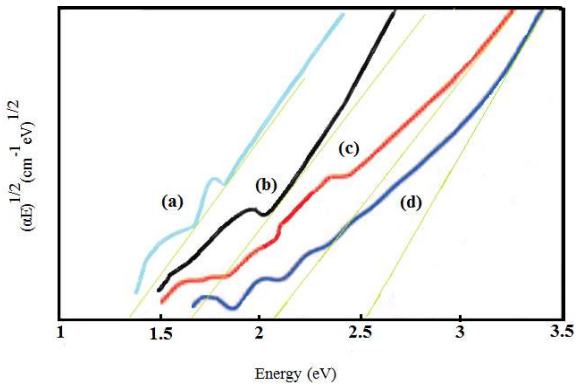

Figure 8. The band gap values of TiN thin films annealed at different temperatures, (a) 400°C, (b) 500°C, (c) 600°C and (d) 700°C.

3.5 Resistivity

The effect of annealing temperature on the electrical characteristics of deposited TiN thin films has been studied by the four-point probe technique at room temperature. The most important aspect in the electronic application of thin films is the resistivity value. The electrical resistivity, (ρ), is strongly influenced by the growth conditions. It is mostly determined by the stoichiometry [63], film thickness [64], temperature (thermal vibrations), intrinsic properties, and defects. At different post annealing temperatures, a change in microstructure, phase composition and defects (grain boundaries, dislocations and impurities) cause changes in the electrical resistivity value [6].

The electrical resistivity values are shown in Table 2. TiN is known as a good conductor with a relatively low electrical resistivity of 25 μΩ-cm [65]. The film annealed at higher temperature, exhibited lower electrical resistivity than other samples. Generally, the increase of post annealing temperature leads to lower defect density, interstitials or vacancies in the TiN thin films which result in increasing the electrical conductivity value.

Furthermore, increasing the grain size during the post annealing treatment leads to decrease in the electron scattering, hence, the films conductivity increases [66]. Ponon et al. [67] reported a similar behavior for annealed TiN thin films.

Table 2. Resistivity and hardness values of TiN films annealed at different annealing temperatures.

Annealing temperature (°C)	Electrical resistivity (μΩ-cm)	Hardness (GPa)
400	84.9	14
500	78.3	13
600	71.7	11
700	67.4	9

Generally, the electrical resistivity value of TiN thin films is less than pure Ti thin films owing to intersection of the Ti 3d electrons of the valence band with the Fermi level [68]. But in our study, the electrical resistivity of the TiN thin film is higher than a pure Ti thin film

because of the polycrystalline nature of our thin films. In polycrystalline TiN, the grain boundary scattering is the most important parameter for increasing the electrical resistivity value [69].

3.6 Hardness

The mechanical properties of deposited thin films are attributed to film structure, microstructure, and composition that are affected by the processing conditions. In transition metal compounds, the mechanical properties like hardness value depends on the chemical bond of atoms and cohesion energy that normally relates to the covalent character of the bonding [70].

Table 2 shows the hardness values of the annealed TiN films at various temperatures. With increasing the post annealing temperature, the hardness value decreases. Generally, the thin film hardness increases when the surface roughness value decreases [49].

Saoula et al. [71] reported that the increase in the thin film hardness value is correlated with decreasing the crystallite size. Vaz et al. [72] reported that the hardness values are related to several parameters such as; phase formation, composition, lattice distortions, (structural defects) and intrinsic stresses.

4 Conclusions

TiN thin films were deposited by using DC magnetron sputtering technique on Si and quartz substrates and their structural and optical properties were characterized after post annealing treatment at different temperatures. According to our experimental study, the post-deposition annealing temperature significantly affects the structures, morphologies, reflection spectra, and band gap energy values of the thin films. The XRD results showed that the amorphous TiN films turned to crystalline structure during thermal treatment. At lower annealing temperatures, TiN films develop a single phase with (111) preferred orientation while, with increasing the annealing temperature, the crystallinity improved and the polycrystalline structure was observed. It is noted that the preferred growth orientation is changed to (220) at higher annealing temperature. The surface morphology of the thin films strongly depends on the annealing temperature. SEM images indicate a significant variation in morphology, a very compact structure changes to a TiN-denuded zone. With increasing the post annealing temperature, TiN films show an increase of reflection in the infrared region. It is found that, by control of the annealing temperature, the optical band gap energy increases, while the hardness and electrical resistivity values decrease.

Acknowledgments

We thank West Tehran Branch Azad University for financial support of this article.

References

[1] D. Jianxin, L. Aihua. “Dry sliding wear behavior of PVD TiN, $Ti_{55}Al_{45}N$, and $Ti_{35}Al_{65}N$ coatings at temperatures up to 600 °C.” International Journal of Refractory Metals and Hard Materials, **41** (2013) 241.

[2] D. Jianxin, W. Fengfang, L. Yunsong, X. Youqiang, L. Shipeng, “Erosion wear of CrN, TiN, CrAlN, and TiAlN PVD nitride coatings.” International Journal of Refractory Metals and Hard Materials, **35** (2012) 10.

[3] P. Hedenqvist, M. Bromark, M. Olsson, S. Hogmark, E. Bergmann, “Mechanical and tribological characterization of low-temperature deposited PVD TiN coatings.” Surface and Coatings Technology, **63** (1994) 115.

[4] T. Polcar, T. Kubart, R. Novák, L. Kopecký, P. Široký, “Temperature dependence of tribological properties of MoS_2 and $MoSe_2$ coatings.” Surface and Coatings Technology, **193** (2005) 192.

[5] A. S. Ingason, F. Magnus, J. S. Agustsson, S. Olafsson, J. T. Gudmundsson, “In-situ electrical characterization of ultrathin TiN films grown by reactive dc magnetron sputtering on SiO_2.” Thin Solid Films, **517** (2009) 6731.

[6] L. Haiyi, L. Yongzhi, G. Bingxiang, X. Liqiang, “Highly (200)-Preferred Orientation TiN Thin Films Grown by DC Reactive Magnetron Sputtering.” American Journal of Physics and Applications, **5** (2017) 41.

[7] A. B. Mei, A. Rockett, L. Hultman, I. Petrov, J. E. Greene, "Electron/phonon coupling in group-IV transition-metal and rare-earth nitrides." Journal of Applied Physics, **114** (2013) 193708.

[8] H.cS. Seo, T. cY. Lee, I. Petrov, J. E. Greene, D. Gall, "Epitaxial and plycrystalline HfNxHfNx (0.8⩽x⩽1.5)(0.8⩽x ⩽1.5) layers on MgO(001): Film growth and physical properties." Journal of Applied Physics, **97** (2005) 083521.

[9] T. Reeswinkel, D. G. Sangiovanni, V. Chirita, L. Hultman, J. M. Schneider, "Structure and mechanical properties of TiAlN–WNx thin films." Surface and Coatings Technology, **205** (2011) 4821.

[10] V. Ataibis, S. Taktak, "Characteristics and growth kinetics of plasma paste borided Cp–Ti and Ti6Al4V alloy." Surface and Coatings Technology, **279** (2015) 65.

[11] B. Rauschenbach, J. W. Gerlach, "Texture Development in Titanium Nitride Films Grown by Low-Energy Ion Assisted Deposition." Crystal Research and Technology, **35** (2000) 675.

[12] P. Patsalas, C. Charitidis, S. Logothetidis, "The effect of substrate temperature and biasing on the mechanical properties and structure of sputtered titanium nitride thin films." Surface and Coatings Technology, **125** (2000) 335.

[13] J. H. Huang, K. J. Yu, P. Sit, G. P. Yu, "Heat treatment of nanocrystalline TiN films deposited by unbalanced magnetron sputtering." Surface and Coatings Technology, **200** (2006) 4291.

[14] P.J. Martin, "Ion-based methods for optical thin film deposition." Journal of Materials Science, **21** (1986) 1.

[15] L.E. Koutsokeras, G.M. Matenoglou, P. Patsalas, "Structure, electronic properties and electron energy loss spectra of transition metal nitride films." Thin Solid Films, **528** (2013) 49.

[16] C.A. Dimitriadis, J.I. Lee, P. Patsalas, S. Logothetidis, D.H. Tassis, J. Brini, G. Kamarinos, Characteristics of TiNx/n-Si Schottky diodes deposited by reactive magnetron sputtering, Journal of Applied Physics, **85** (1999) 4238.

[17] D. Sosnin, D. Kudryashov, A. Mozharov, "Investigation of electrical and optical properties of low temperature titanium nitride grown by rf-magnetron sputtering." Journal of Physics: Conference Series, **917** (2017) 052025.

[18] J. M. Wang, W. G. Liu, T. Mei, "The effect of thermal treatment on the electrical properties of titanium nitride thin films by filtered arc plasma method." Ceramics International, **30** (2004) 1921.

[19] E. Santecchia, E. Zalnezhad, A.M.S. Hamouda, F. Musharavati, M. Cabibbo, S.Spigarelli, "Wear resistance investigation of titanium nitride-based coatings." Ceramics International, **41** (2015) 10349.

[20] I. Petrov, P. B. Barna, L. Hultman, J. E. Greene, "Microstructural evolution during film growth." Journal of Vacuum Science and Technology A, **2** (2003) 117.

[21] S. Sedira, S. Achour, A. Avci, V. Eskizeybek, "Physical deposition of carbon doped titanium nitride film by DC magnetron sputtering for metallic implant coating use." Applied Surface Science, **295** (2014) 81.

[22] R. A. Rosu, V. A. Serban, A. I. Bucur, U. Dragos, "Deposition of titanium nitride and hydroxyapatite-based biocompatible composite by reactive plasma spraying." Applied Surface Science, **258** (2012) 3871.

[23] H. O. Pierson: "Handbook of Refractory Carbides and Nitrides, Properties, Characteristics, Processing and Applications." Noyes Publications, New Jersey, 1996.

[24] P. Patsalas, N. Kalfagiannis, S. Kassavetis, "Optical Properties and Plasmonic Performance of Titanium Nitride." Materials, **8** (2015) 3128.

[25] S. PalDey, S. C. Deevi, "Single layer and multilayer wear resistant coatings of (Ti,Al)N: a review." Materials Science and Engineering A, **342** (2003) 58.

[26] J. E .Alfonso, F. Pacheco, C. Moreno, R. Garzon, J. Torres, "Recubrimientos de TiN realizados mediante magnetrón rf." Revista Colombiana de Fisica, **35** (2003) 47.

[27] M. J. Carbonari, J. R. Martinelli, "Effects of hot isostatic pressure on titanium nitride films deposited by physical vapor deposition," Materials Research, **4** (2001) 163.

[28] H. Hamamura, H. Komiyama, Y. Shimogaki, "TiN films prepared by flow modulation chemical vapor deposition using $TiCl_4$ and NH_3." Japanese Journal of Applied Physics, **40** (2001) 1517

[29] J. Zheng, L.v. Yanhong, X.u. "Shusheng, Nanostructured TiN-based thin films by a novel and facile synthetic route." Materials and Design, **113** (2017) 142.

[30] W. Ensinger, B. Rauschenbach, "Microstructural investigations on titanium nitride films formed by medium energy ion beam assisted deposition." Nuclear Instruments and Methids in Physics Research Section B, **80–81** (1993) 1409.

[31] Y. H. Cheng, B. K. Tay, S. P. Lau, H. Kupfer, F. Richter, "Substrate bias dependence of Raman spectra for TiN films deposited by filtered cathodic vacuum arc." Journal of Applied Physics, **92** (2002) 1845.

[32] H. Wang, A. Tiwari, A. Kvit, X. Zhang, J. Narayan, "Epitaxial growth of TaN thin films on Si(100) and Si(111) using a TiN buffer layer." Applied Physics Letters, **80** (2002) 2323.

[33] J. Paulitsch, M. Schenkel, T. Zufraß, P. H. Mayrhofer, W. D. Münz, "Structure and properties of high power impulse magnetron sputtering and DC magnetron sputtering CrN and TiN films deposited in an industrial scale unit." Thin Solid Films, **518** (2010) 5558.

[34] M. Ritala, M. Leskelä, E. Rauhala, J. Jokinen, "Atomic layer epitaxy growth of TiN thin films from TiI_4 and NH_3." Journal of Electrochemical Society, **145** (1998) 2914.

[35] S. Mahieu, D. Depla, "Reactive sputter deposition of TiN layers: Modelling the growth by characterization of particle fluxes towards the substrate." Journal of Physics D, **42** (2009) 053002.

[36] P. Patsalas, C. Gravalidis, S. Logothetidis," Surface kinetics and subplantation phenomena affecting the texture, morphology, stress, and growth evolution of titanium nitride films." Journal of Applied Physics, **96** (2004) 6234.

[37] N. Saoula, K. Henda, R. Kesri, "Influence of Nitrogen Content on the Structural and Mechanical Properties of TiN Thin Films." Journal of Plasma Fusion Research SERIES, **8** (2009) 1403.

[38] S. Hofmann, "Formation and diffusion properties of oxide films on metals and on nitride coatings studied with Auger electron spectroscopy and X-ray photoelectron spectroscopy." Thin Solid Films, **2** (1990) 193.

[39] W. J. Chou, G.P. Yu, J. H. Huang, "Deposition of TiN thin films on Si(100) by HCD ion plating." Surface and Coatings Technology, **140** (2001) 206.

[40] Y. Jeyachandran, S. Narayandass, D. Mangalaraj, S. Areva, J. Mielczarski, "Properties of titanium nitride films prepared by direct current magnetron sputtering." Materials Science and Engineering A, **445-446** (2007) 223.

[41] G. Gagnon, J. Currie, C. Beique, J. Brebner, S. Gujrathi, L. Onllet, "Characterization of reactively evaporated TiN layers for diffusion barrier applications." Journal of Applied Physics, **75** (1994) 1565.

[42] K. Vasua, M. G. Krishna, K. "Padmanabhan, Substrate-temperature dependent structure and composition variations in RF magnetron sputtered titanium nitride thin films." Applied Surface Science, **257** (2011) 3069.

[43] X. Kewei, C. Jin, G. Rensheng, H. Jiawen, "Therm/al effects of residual macro stress and micro strain in plasma-assisted CVD TiN films." Surface and Coatings Technology, **58** (1993) 37.

[44] P. H. Mayrhofer, F. Kunc, J. Musil, C. Mitterer, "A comparative study on reactive and non-reactive

unbalanced magnetron sputter deposition of TiN coatings." Thin Solid Films, **415** (2002) 151.

[45] M. V. Kuznetsov, M. V. Zhuravlev, E. V. Shalayeva, V. A. Gubanov, "Influence of the deposition parameters on the composition, structure and X-ray photoelectron spectroscopy spectra of Ti N films." Thin Solid Films, **215** (1992) 1.

[46] T. Wierzchon, T. Burakowski, "Surface Engineering of Metals-Principles, Equipment, Technologies." CRC Press, New York, USA, (1999).

[47] James R. Connolly, for EPS 400-001, "Introduction to X-Ray Powder Diffraction." Diffraction Basics, Part 2, Spring 2007.

[48] N. Saoula, S. Djerourou, K. Yahiaoui, K. Henda, R. Kesri, R. M. Erasmus, J. D. Comins, "Study of the deposition of Ti/TiN multilayers by magnetron sputtering." Surface and Interface Analysis, **42** (2010) 1176.

[49] J. P. Zhao, X. Wang, Z. Y. Chen, S. Q. Yang, T. S. Shi, X. H. Liu, "Overall energy model for preferred growth of TiN films during filtered arc deposition." Journal of Applied Physics, D, **30** (1997) 5.

[50] F. Wang, M. Z. Wu, Y. Y. Wang, Y. M. Yu, X. M. Wu, L.J. Zhuge, "Influence of thickness and annealing temperature on the electrical, optical and structural properties of AZO thin films." Vacuum, **89** (2013) 127.

[51] L.K. Robinson, section 10d. Surface specific methods, Methods in materials research, (2000)

[52] K. Vasu, M. G. Krishna, and K. A. Padmanabhan, "Effect of Nb concentration on the structure, mechanical, optical, and electrical properties of nano-crystalline Ti1−x Nb x N thin films." Journal of Materials Science, **47** (2012) 3522.

[53] F. Vaz, L. Rebouta, S. Ramos, M. F. da Silva, J. C. Soares, "Physical, structural and mechanical characterization of Ti1−xSixNy films." Surface and Coatings Technology, **108** (1998) 236.

[54] U. Guler, A. Kildishev, A. Boltassevaab, V. Shalaev, U. Guler, A.V. Kildishev, A. Boltasseva, V. M. Shalaev, "Plasmonics on the slope of enlightenment: the role of transition metal nitrides." Faraday Discussions, **178** (2015) 71.

[55] A. Newport, C. Carmalt, I. Parkin, Shane O'Neill, "Dual source APCVD synthesis of TaN and NbN thin films on glass from the reaction of MCl5 (M = Ta, Nb) and 1,1,1,3,3,3-hexamethyldisilazane." Journal of Materials Chemistry, **14** (2014) 3333.

[56] P. LeClair, G. P. Berera, J. S. Moodera, "Titanium nitride thin films obtained by a modified physical vapor deposition process." Thin Solid Films, **376** (2000) 9.

[57] H. A. Abd El-Fattah, I. S. El-Mahallawi, M. H. Shazly, W. A. Khalifa, Optical Properties and Microstructure of TiNxOy and TiN Thin Films before and after Annealing at Different Conditions, Coatings, **9** (2019) 22.

[58] E. Aydin, M. Sankir, N.D. Sankir, "Influence of silver incorporation on the structural, optical and electrical properties of spray pyrolyzed indium sulfide thin films." Journal of Alloys and Compounds, **603** (2014) 119.

[59] N. Miyata, S. Akiyoshi, Preparation and electrochromic properties of RF-Sputtered molybdenum oxide-films, Journal of Applied Physics, **58** (1985) 1651.

[60] J. Tauc, J. Optical Properties of Solids (North-Holland Pub, Amsterdam, 1972).

[61] S. S. Tneh, Z. Hassan, K. G. Saw, F. K. Yam, and H. A. Hassan, "The structural and optical characterizations of ZnO synthesized using the "bottom-up" growth method." Physica B, **405** (2010) 2045.

[62] A. Kavitha, R. Kannan, P. Sreedhara Reddy, S. Rajashabala, "The effect of annealing on the structural, optical and electrical properties of Titanium Nitride (TiN) thin films prepared by DC magnetron sputtering with supported discharge." Journal of Materials Science: Materials in Electronics, **27** (2016) 10427.

[63] R. Ellwanger, J. Towner, "The deposition and film properties of reactively sputtered titanium nitride." Thin Solid Films, **161** (1988) 289.

[64] Y. Jeyachandran, S. Narayandass, D. Mangalaraj, S. Areva, J. Mielczarski, "Properties of titanium nitride films prepared by direct current magnetron sputtering." Materials Science and Engineering A, **445-446** (2007) 223.

[65] J. E. Sundgren, "Structure and properties of TiN coatings." Thin Solid Films, **128** (1985) 21.

[66] B. Subramanian, R. Ananthakumar, V. S. Vidhya, M. Jayachandran, "Influence of substrate temperature on the materials properties of reactive DC magnetron sputtered Ti/TiN multilayered thin films." Materials Science and Engineering B, **176** (2011) 1.

[67] N. K. Ponon, D. J. R. Appleby, E. Arac, P.J. King, S. Ganti, K. S. K. Kwa, A. O'Neill, "Effect of deposition conditions and post deposition anneal on reactively sputtered titanium nitride thin films." Thin Solid Films, **578** (2015) 31.

[68] M. S. R. N. Kiran, M. G. Krishna, K. A. Padmanabhan, "Substrate-dependent structure, microstructure, composition and properties of nanostructured TiN films." Solid state communications, **151** (2011) 561.

[69] F. Cemina, D. Lundin, D. Cammilleri, T. Maroutian, P. Lecoeur, T. Minea, "Low electrical resistivity in thin and ultrathin copper layers grown by high power impulse magnetron sputtering." Journal of Vacuum Science and Technololy A, **34** (2016) 051506.

[70] F. Le´vy, P. Hones, P.E. Schmid, R. Sanjine´s, M. Diserens, C. Wiemer, "Electronic states and mechanical properties in transition metal nitrides." Surface and Coating Technology, **120** (1999) 284.

[71] N. Saoula, K. Henda, R. Kesri, "Influence of Nitrogen Content on the Structural and Mechanical Properties of TiN Thin Films." Journal of Plasma Fusion Research SERIES, **8** (2009) 1403.

[72] F. Vaz, J. Ferreira, E. Ribeiro, L. Rebouta, S. Lanceros-Me´ndez, J.A. Mendes, E. Alves, Ph. Goudeau, J.P. Rivie`re, F. Ribeiro, I. Moutinho, K. Pischow, J. de Rijk, "content on the structural, mechanical and electrical properties of TiN thin films." Surface and Coatings Technology, **191** (2005) 317.